Sensor Fusion of GPS and Accelerometer Data for Estimation of Vehicle Dynamics

M A T S   M A L M B E R G

Master of Science Thesis
Stockholm, Sweden 2014

Sensor Fusion of GPS and Accelerometer Data for Estimation of Vehicle Dynamics

MATS MALMBERG

Abstract

Connected vehicles is a growing market. There are currently several such services available, but many of them are constrained in the sense that they are bound to recently produced cars and either expensive or strongly limited in the services that they provide. In this master thesis we investigate the possibility to implement a generic platform that is of low cost and simple to install in any vehicle, but that still has the ability to provide a wide range of services. It is proposed that a crucial step in such a system is to reconstruct the vehicle's kinematics, as this enables the possiblity to developed a wide range of services by feature extraction and interpret the result from a dynamics perspective. A mathematical model that describes how the kinematics can be reconstructed is proposed, and a filter that performs such reconstruction is implemented. Based on this reconstruction, two filters that interpret the output are implemented as a proof of concept for the proposed mathematical model. The complete implemented filter solution is tested on measurement data from actual driving scenarios and it is seen that we can identify when the vehicle makes a hard turn, and find where the surrounding road conditions are poor.

Keywords: sensor fusion, connected car, real time filtering

Sammanfattning

Uppkopplade fordon är en växande marknad. I dagsläget finns flera sådana tjänster, men ofta är dessa begränsade i den meningen att de antingen endast finns tillgängliga för nyproducerade fordon eller bara erbjuder ett smalt utbud av tjänster. I detta examensarbete undersöker vi möjligheten att utveckla en generisk plattform för uppkopplade fordon som är billig och enkel att installera, men som också kan erbjuda ett stort urval av tjänster. Det föreslås att ett viktigt steg i en sådan lösning är att rekonstruera fordonets kinematik, då detta möjliggör utvecklandet av ett brett urval av tjänster genom att identifiera karakteristiska egenskaper i kinematiken, samt göra tolkningar utifrån dynamikbetraktelser. En matematisk modell för att beskriva hur kinematiken kan rekonstrueras från givna indata presenteras, och ett filter som utför denna rekonstruktion implementeras. Ytterligare två filter implementeras för att påvisa att den rekonstruerade kinematiken samt den föreslagna matematiska modellen kan användas till att identifiera olika scenarion ur verkligheten. Den kompletta filterlösningen testas på mätdata från faktiska körningar och vi ser att vi kan identifiera när fordonet gör skarpa svängar, samt när vägförhållandena är dåliga.

Nyckelord: sensorfusion, uppkopplade fordon, realtidsfiltrering

Contents

List of Figures

List of Abbreviations

BF   Body Frame
ECEF   Earth Centered Earth Fixed
ISO   International Organization for Standards
M2H   Machine to Human
M2M   Machine to Machine
OEM   Original Equipment Manufacturer
RF   Reference Frame
TEM   Telematic Unit

1. Introduction

Many everyday objects contain one or several, usually quite capable, embedded computers. It is also common that they are programmed to act intelligently on their environment in some way. Most such devices are only acting locally, requiring a human to interact with the device in order to make use of its capabilities. As components become smaller and more capable, the possibilities increase. One trend is to enable connectivity for such everyday objects to a network. It is only a matter of time before the functionality is further extended so that they will be able to communicate and interact with each other, even without the need of human intervention [1]. This prediction suggests that we are entering a new era where everything will or could be connected, thus being able to provide services that are even more intelligent. The vision as a whole is sometimes called *the internet of things*. There is a distinction between devices sharing information from *machine to human* (**M2H**), and devices communicating without human intervention but from *machine to machine* (**M2M**). In practice these concepts overlap in the sense that devices usually provide both M2M and M2H services. For simplicity we will use M2M when talking about connected services, but it is understood that this is not meant in an exclusive way.

A necessity to provide an M2M solution is of course that there is a means of communication, a network. The cellullar network provides a good network infrastructure for connectivity, and an end point of an M2M solution using this type of network is called a *telematic unit* (**TEM**). TEMs can come in various formats and shapes, the shared property is that they can send and receive data over cellullar network. It is common that a TEM device also is equipped with a set of sensors, either internal or external, as well as several input and output connections.

One particular domain where there is an interest of connecting devices is within the car industry. There is a lot of information that could be obtained by a M2M solution, in order to provide usefull services. At a micro level, information about a particular car could be provided to the owner. This could be used to provide sercies such as reading the current status of the car, "pay as you drive" insurance, positioning, etc. At a macro level, information from a large set of cars can be provided to relevant stakeholders. This could be used to provide services on current road conditions, traffic conditions, fleet management etc. There are several existing M2M solutions for connected cars, but they are either bound to a specific brand or have a very limited fuctionality. In this report we will investigate the possibilities to collect and interpret data obtained by a TEM unit installed in a car. This is an important building block to provide a generic, widely functional, connected car solution.

2. Background and Problem Formulation

2.1   The Principal

The thesis is conducted at Springworks AB. Springworks is a technology partner located in Stockholm that specializes in advanced mobile solutions, focusing on business value and usability. They are experienced in working with the automotive industry within the domain of connecting vehicles. The company has developed an M2M platform solution that enables the possibility to connect a large set of TEMs and distribute the obtained data to a relevant end user. The platform is generic and is thus not dependent on the particular TEM chosen, although for this particular study the hardware is fixed.

2.2   The Software Platform Provided

One of the main features of the M2M platform provided by Springworks is the generic nature of their solution. Any car can be connected with the current setup, without an extensive installation procedure. A simplified visual representation of the platform is provided in figure 2.1. A TEM is installed in a car, collecting relevant sensor data. The obtained sensor data can be processed locally on the TEM and the resulting data is sent to a server over the GSM protocol provided by a telecom company. The server then provides an authorized end user with the relevant information. The current platform provides the infrastructure necessary in order to deliver M2M services to an end user. More specifically, it provides the formalism on how to *collect* and *transmit* data. It does not determine *what* data to collect and *how* to interpret it. The context of this thesis is to investigate these questions and to further extend the information available for service development.

As one of the main features of the current platform is the possibility to install it in any type of car, the services must be built on something that is common for all vehicles. The general problem is thus really to indentify such quantities and investigate if they can be measured accurately enough to develop a wide suite of services. Our hypothesis is that the kinematics and the dynamics of the car are such phenomena. With a sufficient knowledge of the kinematics and dynamics of the car, we can analyze patterns and interpret irregularities. Many interesting services are in various ways related to the position, velocity and acceleration of the car.
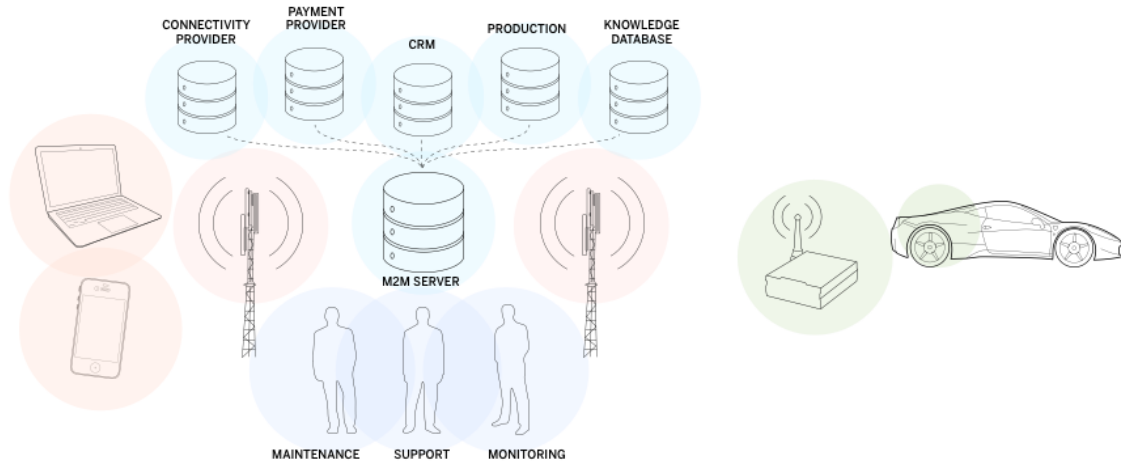
Figure 2.1: M2M plattform provided by Springworks

2.3 Problem Formulation

The main topic of this report is to investigate if we can reconstruct the kinematics from available sensor data and draw any conclusions based on the obtained results, as this would be an important part of the complete system solution. Hence we will investigate the possibility of solving two well defined special cases by interpreting the sensor data provided by the TEM. The problem formulation of this report is thus:

Investigate the possibility to implement a software that can

- *identify where road conditions are bad*

- *give an indication on where the driver has made a hard turn.*

If we can find solutions to these special cases, then evidently there are some micro and macro events that can be solved with the current setup. We also note that the problem formulation, as it stands, is not necessarily bound to be implemented locally on the TEM.

3. Hardware Capabilities and Acquisition of Data

The recieved indata is constrained by the technical limitations of the hardware. In this section we will thus present and discuss the capabilities of the TEM unit. A conclusion is that the available positional measurements are considered planar, due to inaccuray in height data. We also present how a data set of specific test scenarios have been acquired.

3.1 Hardware Capabilities

3.1.1 Technical Specifications for the TEM Unit Used

The TEM used in this project is provided by an external OEM company, and is called CX1 pro-c [2]. It is equipped with an external GPS reciever and an internal three axis accelerometer. The specifications provided by the manufacturer is given in table 3.1 [1].

Gps		Accelerometer		Computational	
Sampling frequency	1Hz	Sampling frequency	100 Hz	CPU frequency	48 MHz
Accuracy	<2,5 m	Resolution	$1 \cdot 10^{-3} \ m/s^2$	Storage capacity	8 GB
Datum	WGS84	Range	$\pm 16 \ m/s^2$	RAM	1088kB

Table 3.1: Technical specifications for CX1 pro-c

To put the given sample rates in a context, consider an emergency brake situation; a car moving at a velocity of 14 m/s (approximately 50 km/h) stops abruptly by decelerating until standing still over 2 seconds (approximately $7m/s^2$ deceleration on average). When comparing sample rates of the hardware with changes in the measured physical quantities over time, it is motivated to say that the GPS is a *low frequency sensor* and the accelerometer is a *high frequency sensor*.

3.1.2 Constraints Inherent to the Hardware

To develop software on the TEM there is a standard library of functions provided by the manufacturer. The functionality provided by this library was deemed to be limited in order to develop a sufficient software within the given time frame of this report. Instead it was decided to collect measurement data from a set of test scenarios and store this into logfiles. With this approach each scenario could be played offline in MATLAB, simulating the sampling procedure. The benefit of this procedure is twofold; firstly, MATLAB provides a more extensive library of functionality which simplifies development of software. Secondly, different software implementations can be tested several times and compared on the exact same indata.

---

[1]The manufacturer uses non standard units, these are here standardized to SI-units.

Usually hardware sensors need to be calibrated in order to yield a precise measurement (see, e.g. [3]). However, calibration is a large topic in its own right and out of scope for this report. We will thus assume that the hardware is calibrated and that the obtained measurements can be trusted. There is one exception to this assumption, namely the height data obtained from the GPS. The obtained test data was verfied for feasibility by a comparison with google maps. This comparison revealed a severe difference in the height data. The anomaly was irregular and the height data obtained by the TEM is thus considered unreliable. As a consequence we will only use the planar longitude and latitude coordinates.

3.2   Acquisition of Data

A TEM unit was installed in a car to collect data from different driving scenarios. Each scenario was driven six times in total, three times at an average velocity of 30 km/h and three times at an average velocity of 50 km/h. The test scenarios were chosen so that the complete test data set would contain a wide variety of features, ranging from normal driving to aggressive driving. Each scenario is briefly described below:
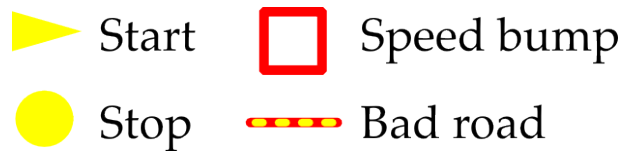
Figure 3.1: Definition of markings for scenarios 1-5

Scenario 1   consists of a fairly straight road section. The purpose of this scenario is to specifically investigate how the system behaves when the driver suddenly hit the brakes. In this scenario the vehicle is accelerated quickly to the predetermined velocity. Once the desired velocity has been reached, the driver hit the brakes hard until the car stops. The road conditions are good and the road has a downhill slope.
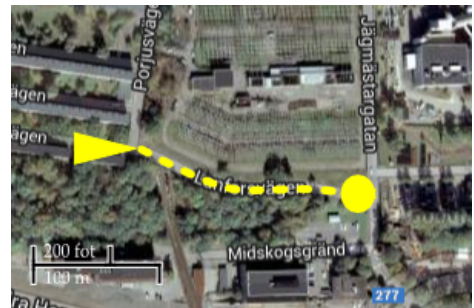
Figure 3.2: Map of test scenario 1

Scenario 2   consists of a straight road with good road conditions and a speedbump. The purpose of this scenario is primarily to investigate how the system reacts when a speedbump is encountered.
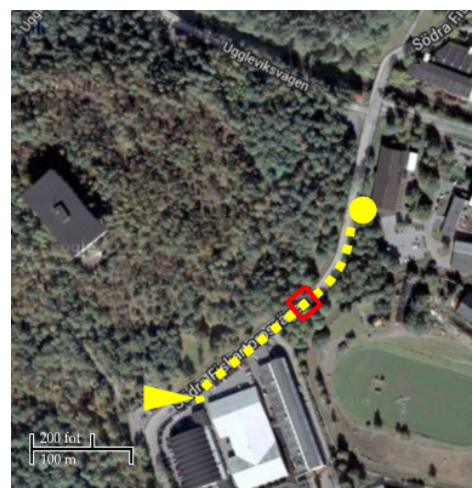
Figure 3.3: Map of test scenario 2
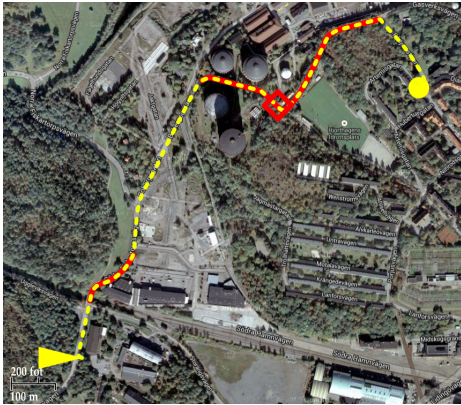
Figure 3.4: Map of test scenario 3

Scenario 3 consists of a relatively long drive with a wide range of possible events. The purpose of this scenario is to illustrate events that may occur when driving normally, thus it contains both good and bad road conditions, potholes, a speedbump, one particularily sharp turn and several normal turns.
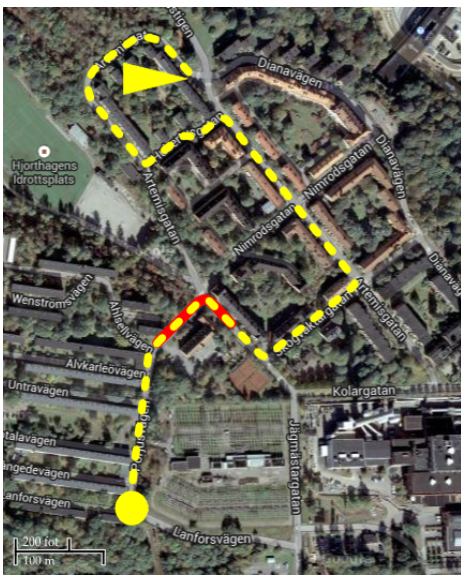
Figure 3.5: Map of test scenario 4

Scenario 4 consists of several hard turns. The purpose of this scenario is to explicitly investigate how the system reacts on hard turns. The road conditions are mostly good, appart from a small section with a road construction site.

Figure 3.6: Map of test scenario 5

Scenario 5 consists of a long road section with very bad road conditions. The purpose of this scenario is to investigate if the system still behaves properly when there are strong disturbances. The road is a gravelled road, with several potholes and a combination of sharp and normal turns.

4. Mathematical Model of Sensor Data

As mentioned in the previous section, the positional measurements of the car are planar. The consequence of this is that we are restricted to a planar model of the car's trajectory. There will still be information in the vertical direction, as the accelerometer has three axes. In this section we will formulate a model of the car and define some necessary concepts related to this model.

4.1   Rigid Body Model of a Car

A car is a suitable system to model with rigid body dynamics. An extensive description on how to apply such theory is provided in [4] and [5] , here we will assume that the reader is somewhat familiar with the concepts and thus present the main results without derivation.
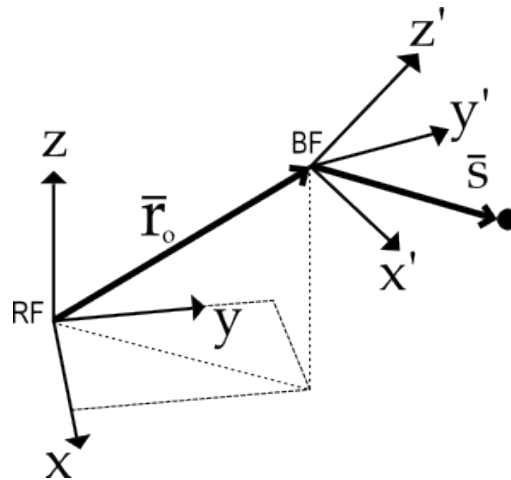
Figure 4.1: Standard coordinate frames in rigid body dynamics

In rigid body dynamics there are two coordinate systems defined. We have a fixed coordinate system, called the *reference frame* (RF) and we have a coordinate system attached to the rigid body called the *body frame* (BF). In general the rigid body is free to move and rotate in space. For any particular point $\bar{\mathbf{s}}$ in BF, the acceleration from the kinematics of the body is a combination of the translational acceleration of the origin in BF and the rotation of the body. This is described by the rigid body equations of motion:

$$
\begin{aligned}
\bar{\mathbf{r}} &= \bar{\mathbf{r}}_o + \bar{\mathbf{s}} \\
\dot{\bar{\mathbf{r}}} &= \dot{\bar{\mathbf{r}}}_o + \bar{\omega} \times \bar{\mathbf{s}} \\
\ddot{\bar{\mathbf{r}}} &= \ddot{\bar{\mathbf{r}}}_o + 2\bar{\omega} \times \dot{\bar{\mathbf{s}}} + \dot{\bar{\omega}} \times \bar{\mathbf{s}} + \bar{\omega} \times (\bar{\omega} \times \bar{\mathbf{s}})
\end{aligned}
\tag{4.1}
$$

Where $\bar{\mathbf{r}}_o$ is the vector to the origin of BF, $\bar{\mathbf{s}}$ is a local vector to the point s expressed in BF and $\bar{\omega}$ is the angular velocity vector, as seen in figure 4.1. Since we only have planar positions available, we will restrict the rigid body's center of mass to planar motion.

The accelerometer installed in the TEM unit measures the net acceleration in a particular point. This is not just the pure accelerations given in equation 4.1, but also gravity and any other external disturbances may be present. We will model the car as a rigid body moving directly above the ground, but with no direct contact. The vibrations resulting from the suspension's interaction with the ground will thus be contained in a noise term. We adopt the following model for the acceleration:

$$\bar{\mathbf{a}}_{measured}(t) = \bar{\mathbf{a}}_{center}(t) + \bar{\mathbf{a}}_{rotation}(t) + \bar{\mathbf{a}}_{gravity}(t) + \bar{\xi}(t). \tag{4.2}$$

Where each term represents

$$
\begin{array}{lll}
\bar{\mathbf{a}}_{measured}(t) & & \text{the acceleration measured by the TEM} \\
\bar{\mathbf{a}}_{center}(t) & = \ddot{\bar{\mathbf{r}}}_o & \text{the center of mass acceleration, from eq. 4.1} \\
\bar{\mathbf{a}}_{rotation}(t) & = 2\bar{\omega} \times \dot{\bar{\mathbf{s}}} + \dot{\bar{\omega}} \times \bar{\mathbf{s}} + \bar{\omega} \times (\bar{\omega} \times \bar{\mathbf{s}}) & \text{the rotational acceleration, from eq. 4.1} \\
\bar{\mathbf{a}}_{gravity}(t) & = [0, 0, -9.82] & \text{the gravitational acceleration, assumed constant} \\
\bar{\xi}(t) & & \text{disturbances such as vibrations and measurement noise}
\end{array}
\tag{4.3}
$$

The purpose of this model is that each of these terms can be interpreted to provide interesting information on the car dynamics. The term $\bar{\mathbf{a}}_{center}(t)$ gives us the necessary information to find the trajectory of the car and the velocity. In general, the term $\bar{\mathbf{a}}_{gravity}(t)$ is not necessarily constant in relation to the car and can be used to find the orientation of the car, as it represents a static reference in RF. The term $\bar{\xi}(t)$ can give indications on the current road conditions, as the interactions between the suspension and the road will be disturbances in the proposed rigid body model.
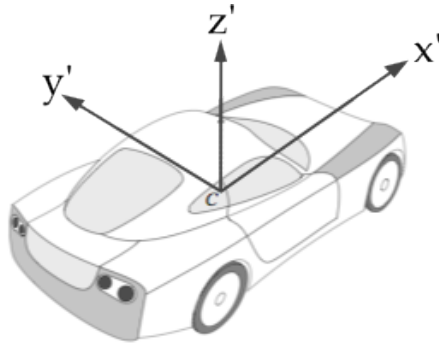
Figure 4.2: The body frame attached to a car

4.2   Defining the Coordinate Systems RF and BF

We will now define the coordinate systems that are used to analyze our rigid body model. The body frame BF is straight forward. It is a carteesian system with its origin at the car's center of mass, as seen in figure 4.2. In general there is also a third coordinate system defined by the axes of the accelerometer. We will assume, without loss of generality, that the accelerometer is aligned with BF. This is no restriction as the alignment is a constant rotation matrix that can be determined when installating the TEM.

Our reference frame RF is constructed based on the standard GPS coordinate system called WGS84 [6]. The foundation of the WGS84 coordinate system is the *reference ellipsoid*, which is an *earth centered earth fixed* (**ECEF**) approximation of the earth's surface. Any point p on the reference ellipsoid is given by its coordinates longitude θ and latitude ϕ. The RF coordinate system is obtained by mapping the ellipsoid surface to a plane, as illustrated in figure 4.3.
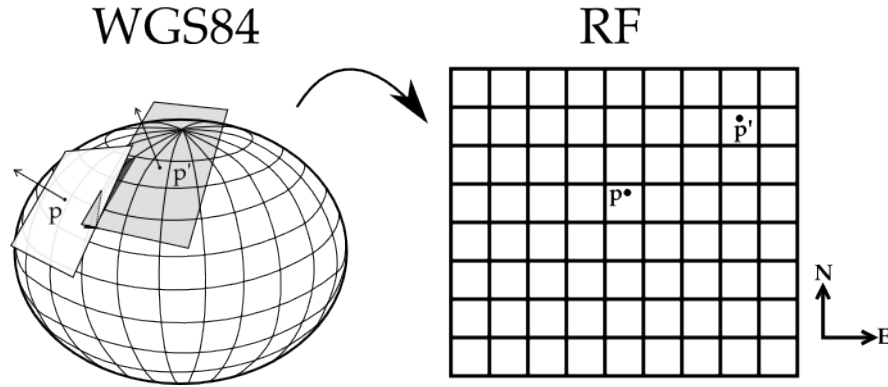
Figure 4.3: The reference frame coordinate system's relation to earth

4.2.1 Longitude and Latitude Coordinates

The reference ellipsoid in WGS84 is defined by its semi and major axis a and b, centered about an ECEF carteesian coordinate system, as illustrated in figure 4.4.
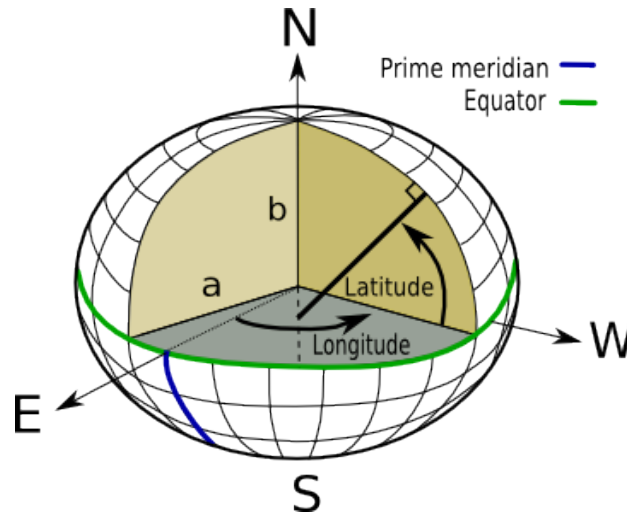
Figure 4.4: Visual representation of the WGS84 reference ellipsoid and coordinates

Let R_N be a line that is normal to the ellipsoid surface and extend this line until it intersects the vertical axis. The angle between the equatorial plane and R_N is the latitude coordinate ϕ. The angle between R_N and the prime meridian axis is the longitude coordinate θ. We emphasize that with this definition, the coordinates are not defined to emanate from the origin.

A consequence of how the coordinates are defined is that in order to analyze distance changes on the surface, we will need to define two radii of curvature. An infinitesimal change in distance in the north and east direction respectively is given by

$$
\begin{aligned}
dN &= R_M d\phi \\
dE &= R_N d\theta
\end{aligned}
$$

(4.4)

In these equations R_N is as previously defined, and is called the radius of the prime vertical. The radius R_M is called the radius of the prime meridian and is the radius of the sphere that is tangent to the ellipsoid at the particular point of interest. We emphasize that both radii will change as a function of the latitude ϕ, and will thus not be constant.

5. Function Definitions

In this section we will present the formal mathematical definitions of how the received input variables $\bar{r}(t)$ and $\bar{a}_{measured}(t)$, representing the measured GPS position and the measured acceleration respectively, are processed in order to provide the sought filter solution. The main idea of the proposed filter is to isolate and identify the quantities describing the dynamics of the car. If this can be done with sufficient precision, many interesting micro and macro event filters can be constructed by identifying features within the kinematics.

5.1   Notation on Different Sample Rates

Both input variables are functions of time, but the sample rates are different. We will use different time variables to clarify and make a distiction between sample rates. So, for an arbitrary function f we define the arguments t, t_m and τ_n to be used in the following way:

$$f(t) \qquad \text{- indicates that the function } f \text{ is time dependent}$$
$$f(t_m) \qquad \text{- indicates that the function is sampled at 1Hz}$$
$$f(\tau_n) \qquad \text{- indicates that the function is sampled at 100Hz}$$

It is assumed that the sampling is synchronized, i.e. that $t_0 = \tau_0$. The indices of the samples are related by the following equation:

$$n = 100 \cdot m + k \qquad k \in \mathbb{N}_{99} \quad n, m \in \mathbb{N} \tag{5.1}$$

Thus the time variable τ_n (of a higher sample rate) is defined for each time sample t_m (of a lower sample rate), but the converse is not true.

5.2   Calculating the Radii of Curvature

An ellipsoid is determined by its semi and major axis. The WGS84 reference ellipsoid is defined in [6], where numerical values of the semi and major axis a and b are given. Formulas to calculate the radius of curvature for the prime vertical and prime meridean respectively are found in [7], these are presented in equations 5.2 - 5.4:

$$e = \sqrt{1 - \frac{a}{b}} \tag{5.2}$$

$$R_N(\phi(t_m)) = \frac{a}{\sqrt{1 - e^2\sin^2(\phi(t_m))}} \tag{5.3}$$

$$R_M(\phi(t_m)) = \frac{a(1 - e^2)}{(1 - (\frac{a}{b}\sin(\phi(t_m)))^{3/2})} = R_N \frac{1 - e^2}{1 - e^2\sin^2(\phi(t_m))} \tag{5.4}$$

5.3 Functions Used to Filter the Data

5.3.1 Kalman Observer Estimate, $\bar{r}(t_m) \to [\bar{p}(t_m), \dot{\bar{p}}(t_m)]^T$

To refine the input signal $\bar{r}(t)$ and to obtain its time derivatives we apply a Kalman filter observer. In the following text we assume that the reader is familiar with the concepts of state space representations of systems and some elementary Kalman filter theory.

The states contained in the state vector $\bar{x}$ consists of the longitude and latitude coordinates as well as their first time derivatives. The vector $\bar{u}$ is the second time derivative of the angular coordinates. Letting $\bar{\omega}$ denote the measurement noise on the output $\bar{y}$, the discrete state space model is given by:

$$
\begin{aligned}
\bar{x}_{m+1} &= \underbrace{\begin{bmatrix} 1 & 0 & 1 & 0 \\ 0 & 1 & 0 & 1 \\ 0 & 0 & 1 & 0 \\ 0 & 0 & 0 & 1 \end{bmatrix}}_{A} \bar{x}_m + \underbrace{\begin{bmatrix} 0.5 & 0 \\ 0 & 0.5 \\ 1 & 0 \\ 0 & 1 \end{bmatrix}}_{B} \bar{u}_m \\
\bar{y}_m &= \underbrace{\begin{bmatrix} 1 & 0 & 0 & 0 \\ 0 & 1 & 0 & 0 \end{bmatrix}}_{C} \bar{x}_m + \underbrace{\begin{bmatrix} 1 & 0 \\ 0 & 1 \end{bmatrix}}_{D} \bar{\omega}_m
\end{aligned}
\tag{5.5}
$$

This system is observable, hence we can apply a Kalman filter observer to obtain refined observations of the states. Furthermore, the system matrices are time invariant the Kalman gain K is constant and can be precalculated. Since the vectors $\bar{u}$ and $\bar{\omega}$ are unknown, we interpret them as disturbances and let R and Q respectively denote their covariance matrices. The Kalman gain is found by solving the equation:

$$
K = APC^T[CPC^T + DRD^T]^{-1},
\tag{5.6}
$$

where P is the unique positive definite solution to the discrete algebraic Riccati equation

$$
P = APA^T - APC^T[CPC^T + DRD^T]^{-1}CPA^T + BQB^T.
\tag{5.7}
$$

Letting $\hat{x}$ denote the Kalman estimate of the state vector $\bar{x}$, the estimates at each sample is given by the recursion

$$
\hat{x}(t_{m+1}) = A\hat{x}(t_m) + K(\bar{r}(t_m) - C\hat{x}(t_m)), \quad \hat{x}(t_0) = [\bar{r}(t_0), 0]^T.
\tag{5.8}
$$

The position output $\bar{p}(t_m)$ and its first time derivative $\dot{\bar{p}}(t_m)$ are defined to be components of the Kalman state estimates

$$
[\bar{p}(t_m), \dot{\bar{p}}(t_m)]^T = \hat{x}^T(t_m).
\tag{5.9}
$$

5.3.2 Solving $\ddot{\bar{p}}(t_m)$ from the Kalman Estimates, $[\bar{p}(t_m), \dot{\bar{p}}(t_m)]^T \to \ddot{\bar{p}}(t_m)$

We note that the acceleration $\ddot{\bar{p}}(t)$ is equal to the vector $\bar{u}$, in equation 5.5. When the recursion given in equation 5.8 is solved, we can thus find $\ddot{\bar{p}}(t_m) = \bar{u}_m$ by rearranging equation 5.5 and solving for $\bar{u}_m$:

$$
B\bar{u}(t_m) = \hat{x}(t_{m+1}) - A\hat{x}(t_m), \quad \ddot{\bar{p}}(t_m) = \bar{u}(t_m).
\tag{5.10}
$$

.

5.3.3   Constructing the Velocity, $\dot{p}(t_m) \rightarrow \bar{v}(\tau_n)$

To find the velocity from the angular velocity $\dot{p}(t_m)$, we first apply a moving median filter. This reduces the amount of outliers in the low frequency input:

$$\dot{p}'(t_m) = \text{median}(\dot{p}(t_{m-r}), \dot{p}(t_{m-r+1}), ..., \dot{p}(t_{m+r-1}), \dot{p}(t_{m+r})). \tag{5.11}$$

Next, we use a linear interpolation to assign $\dot{p}'(\tau_n)$ a value for each τ_n:

$$\dot{p}'(\tau_n) = \dot{p}'(t_m) + k\frac{\dot{p}'(t_{m+1}) - \dot{p}'(t_m)}{100} \tag{5.12}$$

where the n, m and k have the same meaning as in equation 5.1. When we have found $\dot{p}'(\tau_n)$, the final step is to scale into the appropriate unit km/h. Here it is important to use the correct radius of curvature, given by equation 5.3 and 5.4. We arrive at the desired result by the following scaling:

$$\bar{v}(\tau_n) \quad = \quad \left[\begin{array}{cc} 3.6 \cdot R_N(\phi(t_m)) & 0 \\ 0 & 3.6 \cdot R_M(\phi(t_m)) \end{array} \right] \dot{p}'(\tau_n). \tag{5.13}$$

5.3.4   Constructing the Center of Mass Acceleration, $(\ddot{p}(t_m), \bar{v}(\tau_n)) \rightarrow \bar{a}_{center}(\tau_n)$

By applying equation 5.11 and 5.12 with $\ddot{p}(t_m)$ instead of $\dot{p}(t_m)$, we obtain $\ddot{p}'(\tau_n)$. We scale with the appropriate radii:

$$\bar{a}'_{center}(\tau_n) \quad = \quad \left[\begin{array}{cc} R_N(\phi(t_m)) & 0 \\ 0 & R_M(\phi(t_m)) \end{array} \right] \ddot{p}'(\tau_m). \tag{5.14}$$

This gives us the center of mass acceleration, in RF coordinates. We want to transform this into BF coordinates. Hence we must find an appropriate transformation matrix T for each time instance τ_n. This matrix is found by a passive transformation from RF to BF (a rotation matrix rotating clockwise):

$$T(\tau_n) = \left[\begin{array}{ccc} \cos(\alpha_n) & -\sin(\alpha_n) & 0 \\ \sin(\alpha_n) & \cos(\alpha_n) & 0 \\ 0 & 0 & 1 \end{array} \right]^{-1}, \quad \alpha_n = \arctan\left(\frac{v_y(\tau_n)}{v_x(\tau_n)}\right). \tag{5.15}$$

Finally, we obtain the center of mass acceleration $\bar{a}_{center}(\tau_n)$ by:

$$\bar{a}_{center}(\tau_n) = T\bar{a}'_{center}(\tau_n). \tag{5.16}$$

5.3.5   Identifying Noise and Net Acceleration, $\bar{a}_{measured}(\tau_n) \rightarrow (\bar{\xi}(\tau_n), \bar{a}_{net}(\tau_n))$

Using the acceleration model formulated in section 4.1, we define the net acceleration $\bar{a}_{net}(t)$ to be:

$$\bar{a}_{net} = \bar{a}_{center} + \bar{a}_{rotation} + \bar{a}_{gravity}. \tag{5.17}$$

It is evident that we will find $\bar{a}_{net}$ if we eliminate the noise from $\bar{a}_{measured}$. A common assumption on noise is that $\bar{\xi} \in N(0, \sigma^2)$ and that $\bar{\xi}$ has a higher frequency content than the measured quantity. Hence it makes sense to apply a low pass filter. A simple but effective implementation of a low pass filter is the moving average filter, as mentioned in [8]. By our assumption $E(\bar{\xi}) = 0$ it follows that

$$\sum_{i=n-s}^{n+s} \frac{\bar{\xi}(\tau_i)}{2s+1} \rightarrow 0.$$

Assuming that the acceleration components varies slowly, compared to the noise, we thus have that

Function Definitions

$$\bar{a}_{net}(\tau_n) \approx \sum_{i=n-s}^{n+s} \frac{\bar{a}_{measure}(\tau_i)}{2s+1} = \sum_{i=n-s}^{n+s} \frac{\bar{a}_{center}(\tau_i) + \bar{a}_{gravity}(\tau_i) + \bar{a}_{rotation}(\tau_i)}{2s+1} + \sum_{i=n-s}^{n+s} \frac{\bar{\xi}(\tau_i)}{2s+1} \quad (5.18)$$

$$\Rightarrow \bar{a}_{net}(\tau_n) \approx \bar{a}_{center}(\tau_n) + \bar{a}_{gravity}(\tau_n) + \bar{a}_{rotation}(\tau_n). \quad (5.19)$$

And also, as a result we can find the noise $\bar{\xi}$ by

$$\bar{\xi}(\tau_n) = \bar{a}_{measured}(\tau_n) - \bar{a}_{net}(\tau_n) \quad (5.20)$$

5.3.6 Identifying the Rotational Acceleration,
$$\left(\bar{a}_{net}(\tau_n), \bar{a}_{center}(\tau_n), \bar{a}_{gravity}(\tau_n)\right) \rightarrow \bar{a}_{rotation}(\tau_n)$$

When all acceleration terms in our acceleration model except $\bar{a}_{rotation}(\tau_n)$ are known, the final term is found by a simple subtraction:

$$\bar{a}_{rotation}(\tau_n) = \bar{a}_{net}(\tau_n) - \bar{a}_{gravity}(\tau_n) - \bar{a}_{center}(\tau_n). \quad (5.21)$$

6. Proposed Solution

In this section we will describe how the functions presented in the previous chapter are combined to produce the desired result. The main idea of the proposed solution is to isolate and identify each term in the model with the kinematics filter, so that the output data can be analyzed for events. The proposed filter solution is thus a composition of three filters; the kinematics filter, the micro event filter and the macro event filter. The kinematics filter is the core of the proposed filter solution. Its purpose is to reconstruct the kinematics based on the indata obtained by sensors. The micro and macro event filters act on the output from the kinematics filter and analyze if a particular event has occured. This setup can easily be expanded by letting other feature detecting filters act on the output provided by the kinematics filter. The performance of the cascaded filters will however strongly depend on the accuracy of the kinematics filter.

6.1 Filter Components

6.1.1 The Kinematics Filter

The kinematics filter separates the measured data into components and identifies their reading according to the model proposed in section 4.1. The resulting output currently contains more data than we will use in the application at hand. The reason for this redundancy is that we may wish to expand the filter solution, and identify other events. In such future applications we may need to interpret other features than the ones presented in section 6.1.2 and 6.1.3.

The filter operates at approximately a two second lag, as a consequence of the low sample rate on the position. In the following filter description we let t_m denote time instance of the currently handled sample, considered by the filter to be present time, and similarly for the high frequency τ_n. At each sample t_m the filter improves the reading of the position, constructs the velocity and acceleration and interpolates these into a high frequency data set in the following way:

1. Obtain the position $\bar{p}(t_{m+1})$ and its time derivative $\dot{\bar{p}}(t_{m+1})$ by applying a Kalman observer on the input $\bar{r}(t_m)$, given by equations 5.8 and 5.9.

2. Obtain the second time derivative by solving equation 5.10.

3. Refine time derivatives and construct the high frequency interpolations of velocity and center of mass acceleration, by applying equation 5.11-5.13

Simultaneously, the high frequency data $\bar{a}_{measured}$ is being processed on the interval $\tau_n \in [\tau_{n-50}, \tau_{n+50}]$ in the following way:

1. Separate and identify the noise and the net acceleration, contained in the sensor data, by applying equation 5.19 and 5.20

2. Find the linear transformation from RF to BF by applying equation 5.15

3. Find the rotational acceleration term by applying equation 5.21

The resulting output from the kinematics filter is a set of vectors $\{\bar{p}(t_m), \bar{v}(\tau_n), \bar{a}_{center}(\tau_n), \bar{a}_{gravity}(\tau_n),$ $\bar{a}_{rotation}(\tau_n), \bar{a}_{net}(\tau_n), \bar{\xi}(\tau_n)\}$ and a matrix $T(\tau_n)\}$.

6.1.2 The Micro Event Filter

The micro event filter should identify when the features of a hard turn is found in the output data set from the kinematics filter. The feature that we look for is when the amplitude in the lateral acceleration of the car is larger than a certain threshold α. The acceleration of interest for this is $\bar{a}_{center}$, but features could also be found in $\bar{a}_{net}$ since $\bar{a}_{center}$ gives the main contribution. A hard turn also typically has a duration that is longer than one second. The features that characterize hard turns are thus found by the following function:

$$f_{micro}(t_m) = \begin{cases} 1 & \text{if} & \exists \tau_r, \tau_s \in (t_{m-1}, t_m] & \text{such that } |\bar{a}_{center}(\tau_r)| > \alpha \text{ and } |\bar{a}_{net}(\tau_s)| > \alpha \\ 1 & \text{if} & \exists \tau_r \in (t_{m-2}, t_{m-1}], \exists \tau_s \in (t_{m-1}, t_m] & \text{such that } |\bar{a}_{net}(\tau_r)| > \alpha \text{ and } |\bar{a}_{net}(\tau_s)| > \alpha \\ 1 & \text{if} & \exists \tau_r \in (t_{m-1}, t_m], \exists \tau_s \in (t_m, t_{m+1}] & \text{such that } |\bar{a}_{net}(\tau_r)| > \alpha \text{ and } |\bar{a}_{net}(\tau_s)| > \alpha \\ 0 & & \text{otherwise} \end{cases}$$

$$(6.1)$$

Informally, what this says is that if both $\bar{a}_{center}$ and $\bar{a}_{net}$ agree that the lateral acceleration is above the threshold within the time interval then this is to be interpreted as a hard turn. This condition is not sufficient due to inaccuracy in the $\bar{a}_{center}$ variable. Hence we also investigate if the duration of the breach stretches over more than one second in $\bar{a}_{net}$.

6.1.3 The Macro Event Filter

The macro event filter should identify when the features of bad road conditions are found in the output data set from the kinematics filter. It is proposed that a road can be considered bad in two different ways (or a combination of both); either the ground is irregular on a road section, or there are local obstacles such as potholes.

Features that characterize the first type of bad road condition is proposed to be an increased variation on the amplitude. Hence this is identified by variations in noise $\bar{\xi}$ larger than a certain threshold β. We will use the following function to find irregular road features:

$$f_{macro}(\tau_n) = \begin{cases} 1 & \text{if} & Var(\bar{\xi}(\tau_n)) > \beta, \quad \tau_i \in [\tau_{n-w}, \tau_{n+w}] \\ 0 & \text{otherwise} \end{cases}$$

$$(6.2)$$

As the quality of the road decrease, the vibrational noise will increase and at some point it will be visible on all three axes. Hence the certainty that a particular alarm is true will increase if features are found on several axes simultaneous. When collecting data from several cars to find sections where the road is bad, not only the frequency of warnings but also the certainty of each warnings will be useful information.

Features that characterize the second type of bad road conditions is proposed to be sharp peaks that are large in amplitude in relation to neighboring measurements. By investigating the vibrational acceleration data, it is evident that all occuring peaks have an amplitude larger than one. Based on this observation we argue that an inherent feature of peaks representing potholes is that they have an amplitude larger than one. To further enhance this characteristic we square the signal and apply a threshold filter:

$$g_{macro}(t_m) = \begin{cases} 1 & \text{if} & \exists \tau_n \in (t_{m-1}, t_m] \text{ such that } \bar{\xi}(\tau_n)^2 > \gamma \\ 0 & \text{otherwise} \end{cases} \tag{6.3}$$

6.2 Setting Filter Parameters

6.2.1 Threshold α for Micro Events

We need to determine at what amplitude the threshold α should be set. Hence we must quantify what is meant by a hard turn. To this end we consider a ninety degree turn found within scenario 3. By measuring, we find that the radius of curvature for the turn is approximately 30m. Considering the ideal case of planar motion with no other acceleration than the one turning the vehicle, as seen in figure 6.1, the following accelerations are found for different velocities.

Velocity $[km/h]$	30	40	50
Acceleration $[m/s^2]$	2.3	4.1	6.4

At the particular road section the speed limit is 30 km/h. In order to allow for some measurement latitude, we set the threshold for a hard turn to be at $\alpha = 4 \ m/s^2$.
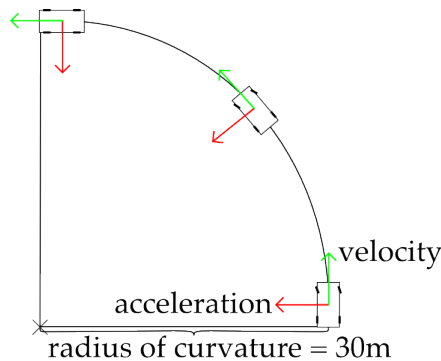
Figure 6.1: Picture illustrating the physical example considered to the determine threshold α

6.2.2 Setting the Thresholds β and γ for Macro Events

To find the normal deviation we investigate the measurement data when the car is at rest with the engine turned on, or driving on road sections where the conditions are known to be good. By such an evaluation on a data set ranging over a total of 7 minutes we find that a normal deviation of noise is $\sigma^2 \approx 0.3902$. To allow some latitude we set the deviation threshold to $\beta = 0.4$.

The threshold γ was found by tuning parameters. If a too low value is used the filter returns false positives, whereas a too high value results in false negatives. An appropriate value was found to be $\gamma \approx 6$.

7. Results

Measurement data was collected from five different scenarios. Each scenario is described in section 3.2. All scenarios were driven and measured at 30 km/h and 50 km/h, three times for each velocity. We will only present a selection of results from scenario 3 and 4, as the features found within these scenarios are considered to be representative and sufficient to illustrate the relevant conclusions for this report.

As mentioned in section 6, the purpose of the kinematics filter is to isolate and identify the components according the the model given in section 4. We will present the results from scenario 3 for two different velocities, as this is considered to contain most of the features that are relevant for our conclusions. Since there is an inifinite set of feasible kinematic curves, nothing can be said about the true correctness based on the presented data. Instead we will comment on reliabilitiy, based on feasibility and the driver's perception.

7.1 The Kinematics Filter

In figure 7.1 we see a trajectory plot of the position output $\bar{p}(t)$, with $\bar{v}(t)$ and $\bar{a}_{center}(t)$ attached to each position as vectors. By comparison, the trajectory is in accordance with the map given in figure 3.4. Relating the positional samples between figure 7.1(a) and figure 7.1(b), we see that they are more sparse when the velocity is increased. We conclude that the positional samples behave as expected.

We observe that the velocity vectors are approximately tangent to the trajectory and that changes are in accordance with the direction of the corresponding acceleration vector. When the velocity is increased, as seen in figure 7.1(b), the difference between consecutive velocity vectors become more apparent. Overall the kinematic quantities presented in figure 7.1 are considered to be physically feasible.
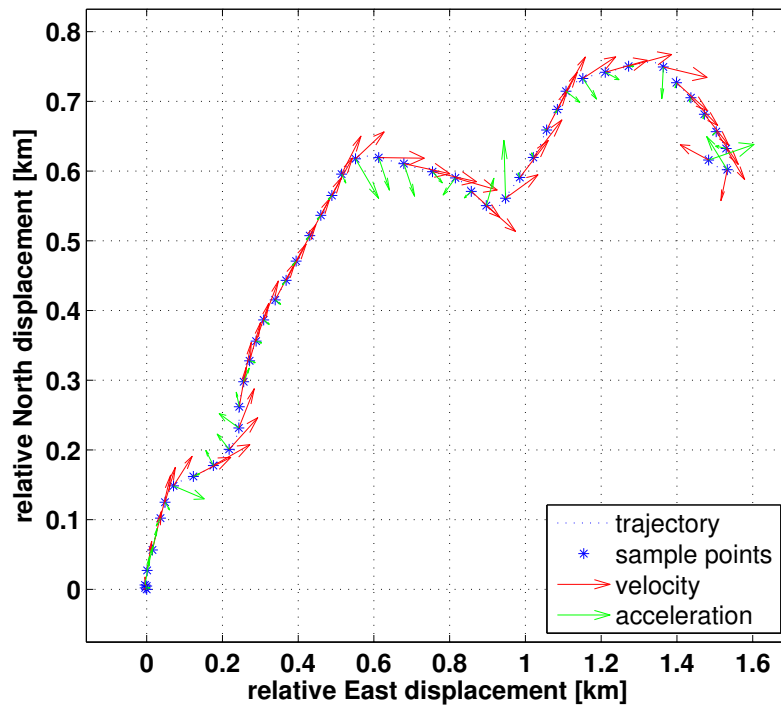
(a) Target average velocity 30 km/h
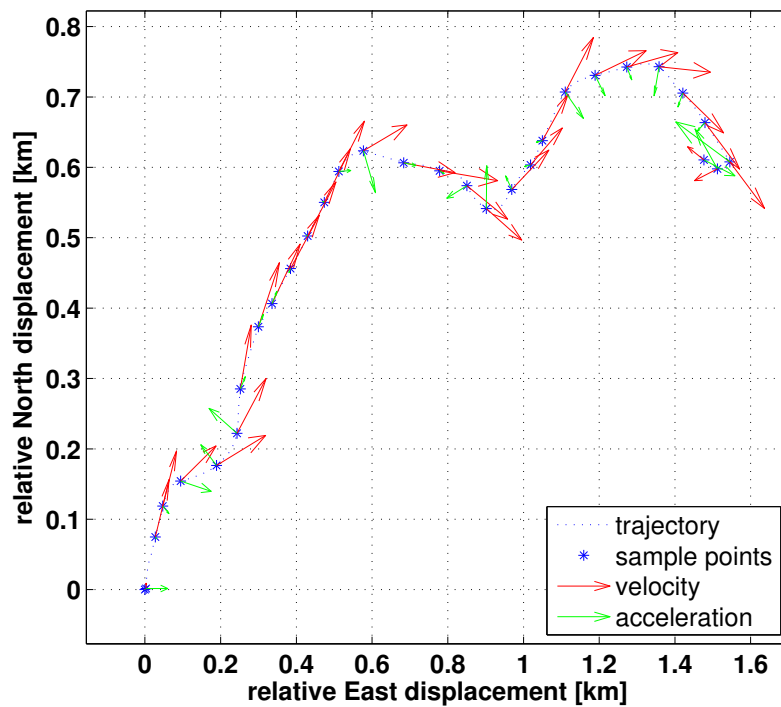
(b) Target average velocity 50 km/h

Figure 7.1: Trajectory of scenario 3 with filter estimates of acceleration and velocity attached to each position sample as vectors.
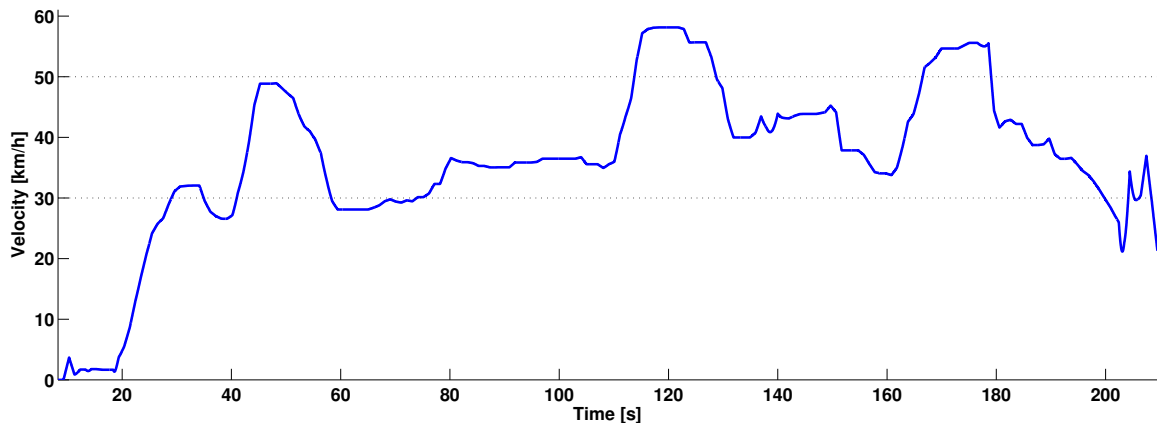
(a) Target average velocity 30 km/h
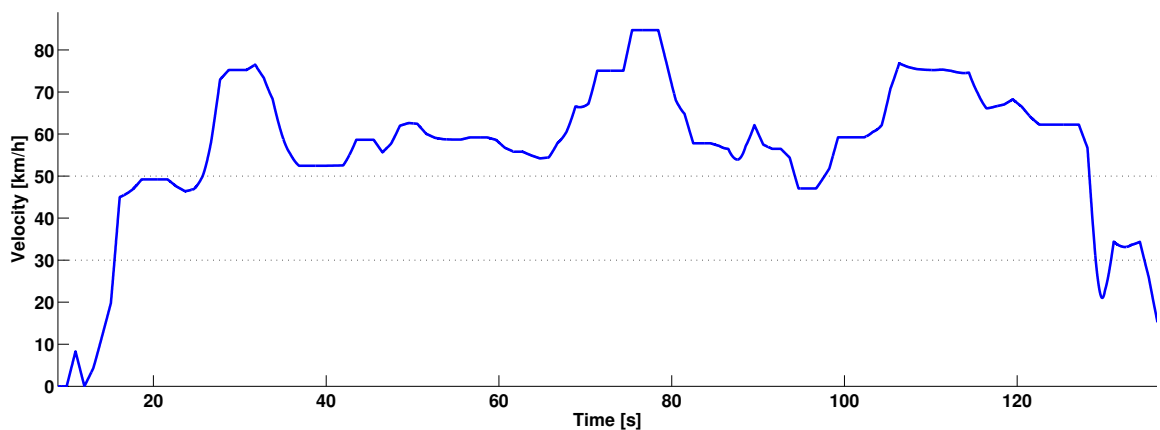
(b) Target average velocity 50 km/h

Figure 7.2: Absolute velocity over time for scenario 3 at two different target velocities.

In figure 7.2 we see two plots of the velocity over time, with reference lines at 30 km/h and 50 km/h. The curves are slightly larger in amplitude than the corresponding reference line at both velocities. Both curves have a similar shape in the sense that they are mainly centered at some average velocity but there are three outliers of relatively large amplitude. Comparing the time of the outliers with the corresponding position samples we observe that they occur at road sections where the trajectory contains a sharp turn. These outliers are erroneous and will be commented further in section 8.1.1

In figure 7.3 the vibrational noise $\bar{\xi}(t)$ is represented component wise in the BF coordinate system. All curves are centered about zero, which is to be expected as we assumed that $\bar{\xi}(t) \in N(0, \sigma^2)$. The curves are similar in their overall appearance, though the time scale is different. This is as expected, as the measurements are taken on the same road section but at different velocities. Furthermore, one can see the features of the bad road section as an increased amplitude of noise at the later part of the data set. Sharp peaks present in the data are restricted to time instances where the surrounding noise amplitudes are relatively large. Interpreting the peaks as potholes or similar obstacles, this is what we would expect as it implies that the potholes are present in road sections of poor quality.
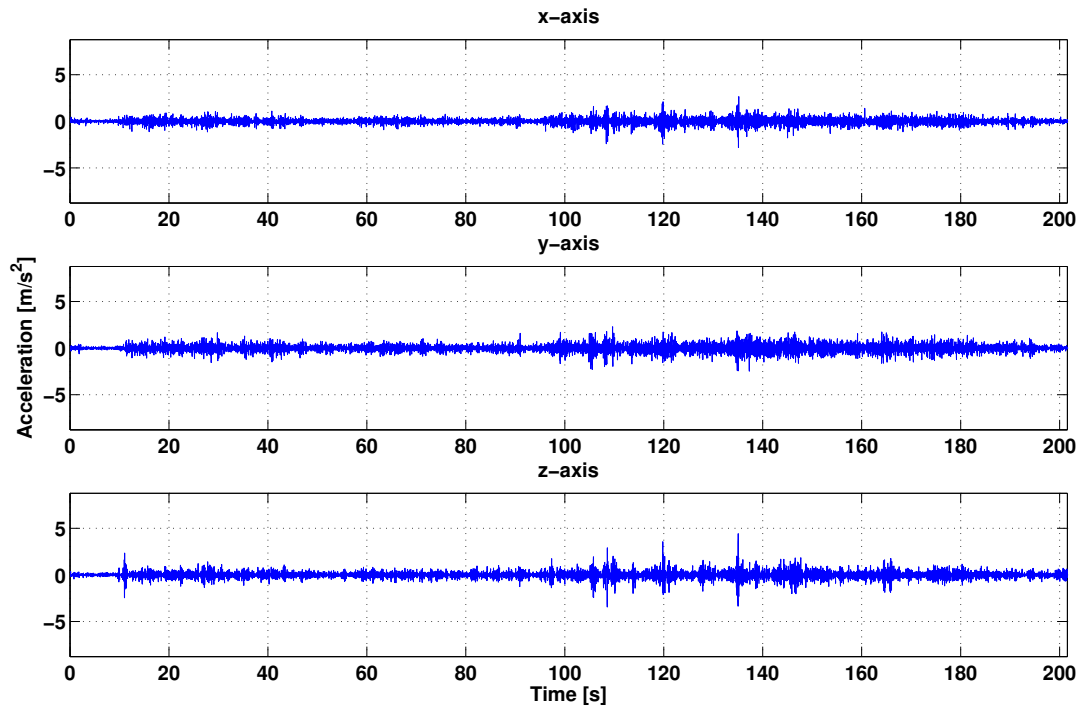
(a) Target average velocity 30 km/h
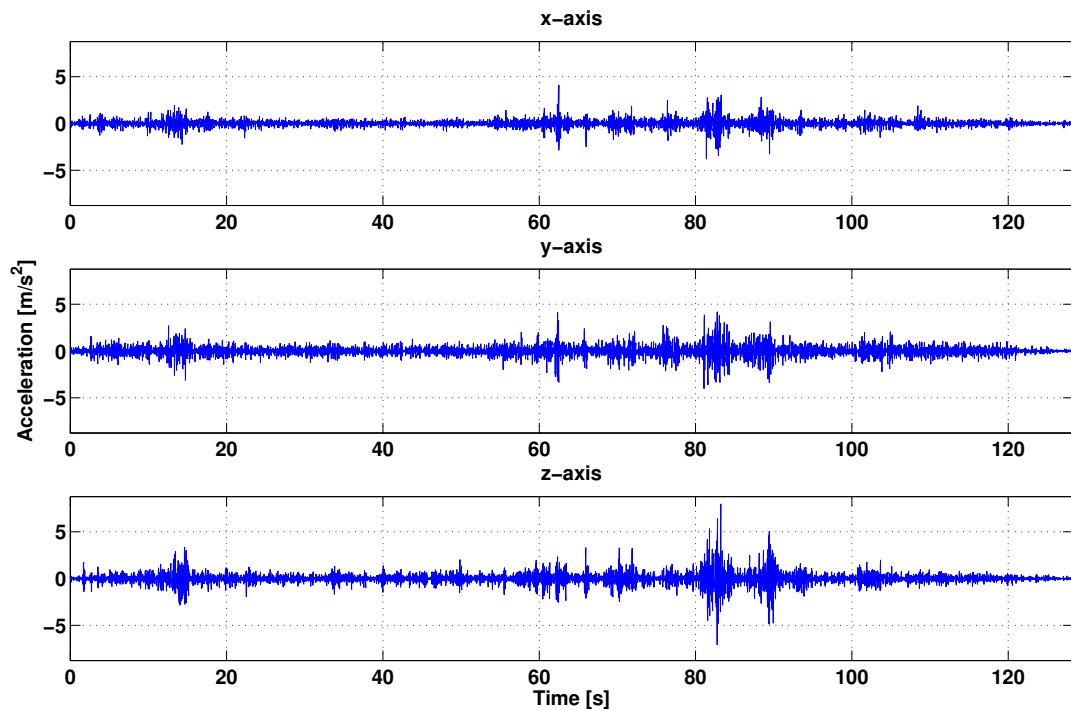
(b) Target average velocity 50 km/h

Figure 7.3: Vibrational acceleration in BF coordinate frame, filtered out from scenario 3 at two different target velocities. The scenario consists of normal driving on a road section with varying road conditions.

In figure 7.4 we see the acceleration output, presented component wise in the BF coordinate system. Overall the curves corresponds well to what we would expect. The x-axis corresponds to the heading direction of the vehicle. A large deviation in the x-direction corresponds to a fast change in velocity, small deviations thus corresponds to smooth car handling. In the x-direction the measured acceleration does not show any large deviations. This is in accordance with what we would expect as it was intended to maintain a constant velocity throughout the scenario. The y-axis corresponds to the lateral acceleration of the vehicle. Deviations in the y-direction corresponds to events that a passenger would percieve as being drawn sideways, examples of such events are fluttering of the car as a result of obstacles or making a turn. Turns can be seen in the lateral data y-axis as relatively smooth deviations that stretch over a longer duration, typically a few seconds. An example of a sharp left turn is seen in figure 7.4(b) at $70 \leq t \leq 80$, and a more subtle right turn is seen in the same figure at $50 \leq t \leq 60$.

In the map for scenario 3 (figure 3.4) we see that there are a total of seven turns, out of which four are considered sharp turns from a geometrical perspective. Considering the y-axis of the measured acceleration in figure 7.4(a), we see features from turns at time instances $t \approx 130$ and $t \approx 190$. In the same manner we see turn features in figure 7.4(a) at time instances $t \approx 15, 25, 55, 75, 105, 120$. Comparing this with the corresponding positional samples, this is what we would expect.

The main contribution to the acceleration of the car should be the acceleration of the center of mass. The curve representing $\bar{a}_{center}(t)$ is observed to differ from the measured acceleration more than we would expect. The acceleration curve for $\bar{a}_{center}(t)$ has several outliers compared to the measured acceleration, especially in the x-direction. The similarity between $\bar{a}_{center}(t)$ and the measurements is better in the y-direction than in the x-direction. The curve representing the rotational acceleration $\bar{a}_{rot}(t)$ is considered to be unfeasible. The rotational accelerations should either be of very short duration, very small amplitude or both.
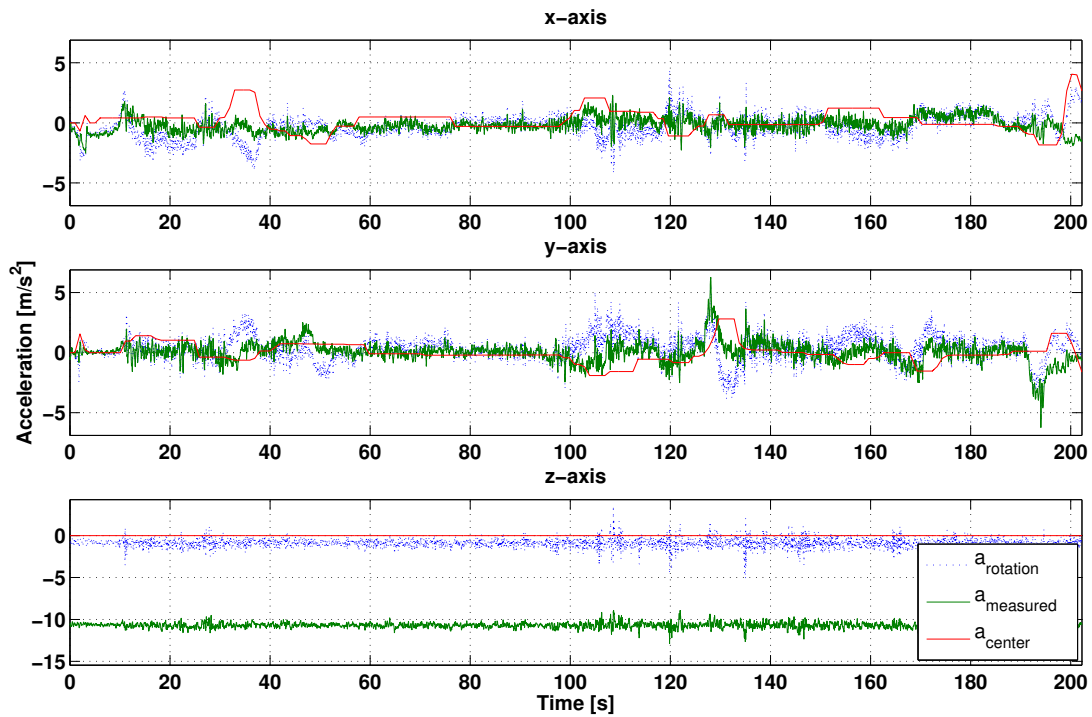
(a) Target average velocity 30 km/h
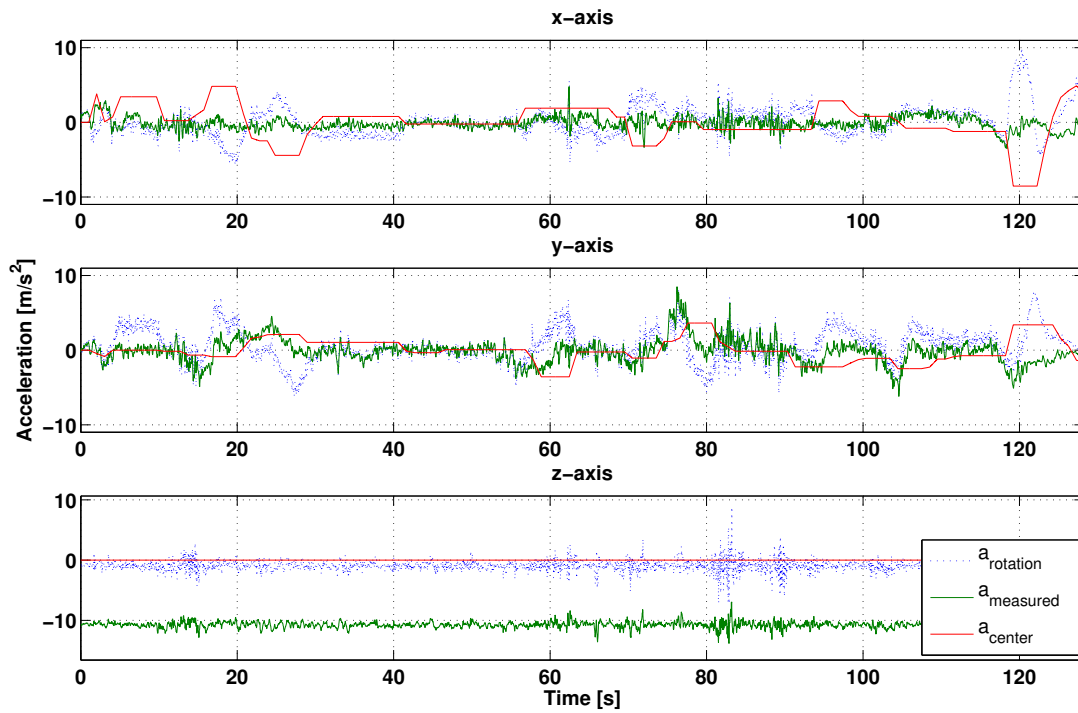
(b) Target average velocity 50 km/h

Figure 7.4: Selection of acceleration curves in BF coordinate system, filtered out at two different target velocities from scenario 3. The scenario consists of normal driving on a road section with varying road conditions.

7.2 The Micro Event Filter

In figure 7.5 and 7.6 we see the positions where sharp turn events have been recognized by the micro event filter in scenario 3 and 4 respectively. For scenario 3, it is seen in figure 7.5(a) that when the average velocity is 30 km/h only two events occur. Both of these events are at positions where road actually makes a sharp turn. In figure 7.5(b), the velocity is increased and the same sharp turns are still recognized but several additional hard turns are recognized. Some of the new warnings are at relatively smooth road sections. In figure 7.5(b) we also see two false positive warnings at a straight road section. We note that this particular road section is of poor quality, which may result in disturbances.
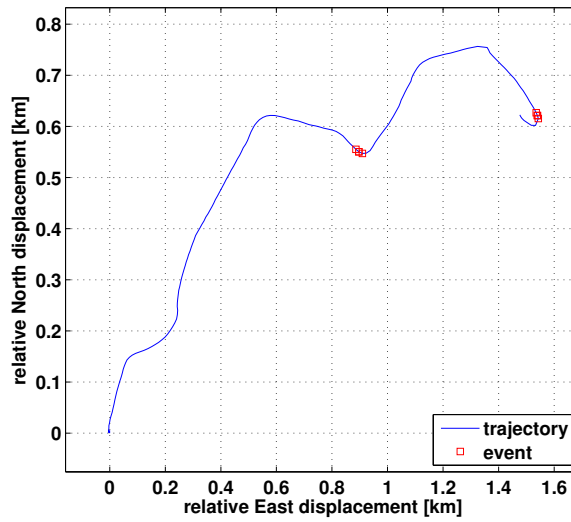
(a) Target average velocity 30 km/h
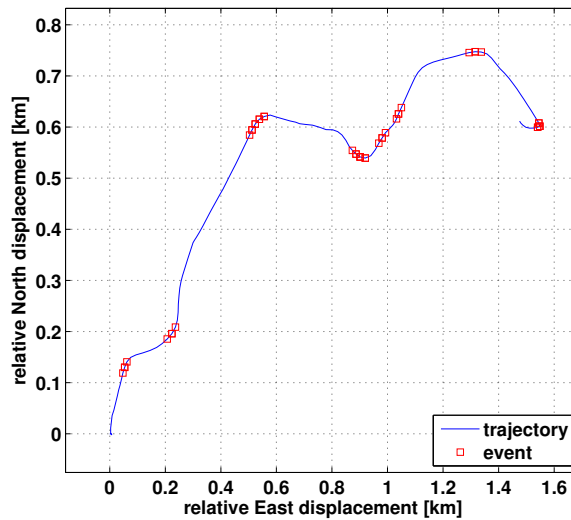
(b) Target average velocity 50 km/h

Figure 7.5: Sharp turn events detected by the micro event filter in scenario 3 at different target velocities. The sharp turn events are marked on the trajectory measured by the GPS.
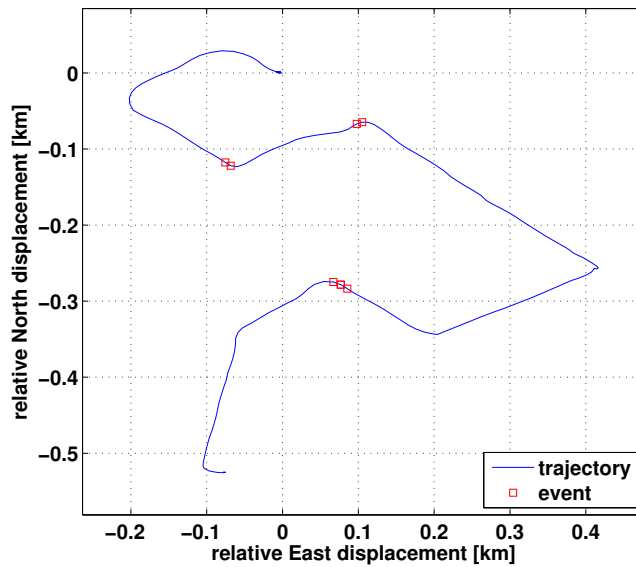
(a) Target average velocity 30 km/h
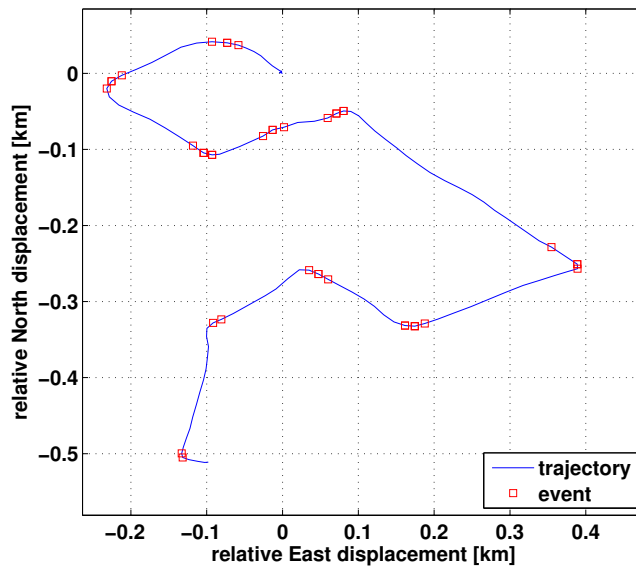
(b) Target average velocity 50 km/h

Figure 7.6: Sharp turn events detected by the micro event filter in scenario 4 at different target velocities. The sharp turn events are marked on the trajectory measured by the GPS.

The events that are obtained for scenario 4 by the micro event filter are seen in figure 7.6(a) and 7.6(b). In figure 7.6(b) there are some events marked on a road section that at first glance seems to be a straight road section. A closer look on the map reveals that this road section really is "s-shaped". We conclude that all of these events are considered to be relevant based on the perception of the driver.

7.3   The Macro Event Filter

In figure 7.7 and 7.8 we see the results obtained from the macro event filter in scenario 3 and 4 respectively. Comparing these results with the scenario descriptions in figure 3.4 and 3.5, we see that the features found are in accordance with what we should expect. In figure 7.7(b) all sections of poor road quality are found, whereas in figure 7.7(a) only the second section is marked.
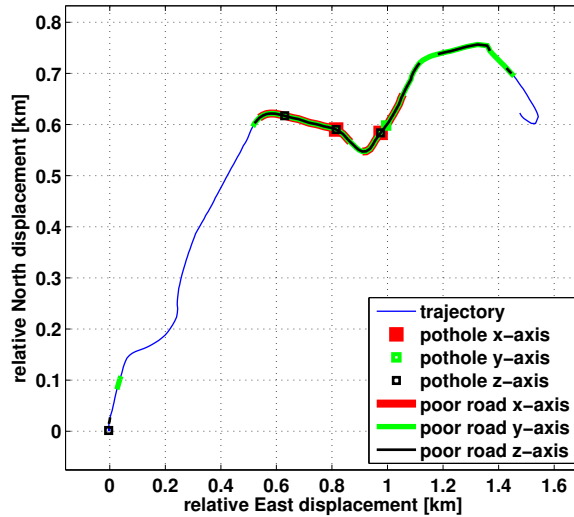
(a) Target average velocity 30 km/h
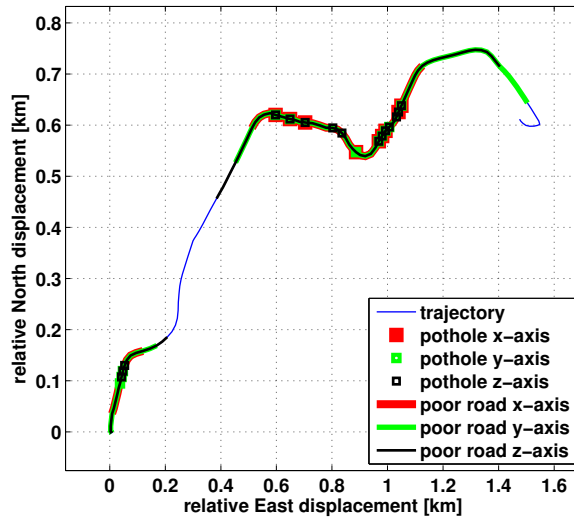
(b) Target average velocity 50 km/h

Figure 7.7: Features of bad road sections found by the macro event filter in scenario 3 at different target velocities. Potholes are marked by squares and poor road quality is marked by a bold line. The thin blue line represents the trajectory measured by the GPS.
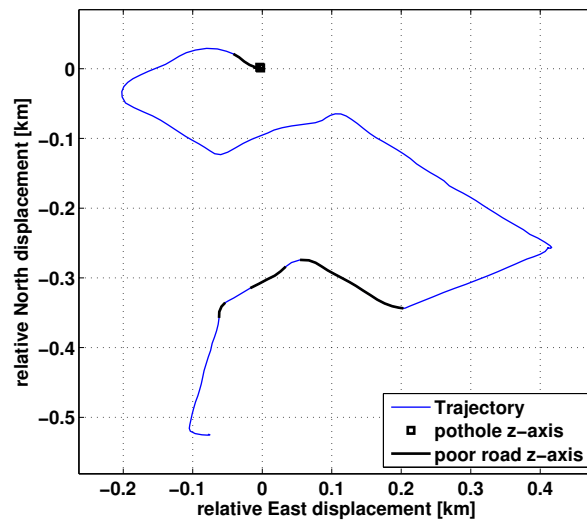
(a) Target average velocity 30 km/h
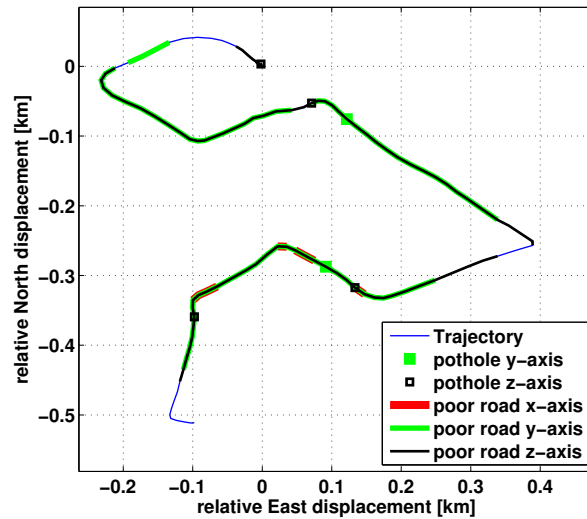
(b) Target average velocity 50 km/h

Figure 7.8: Features of bad road sections found by the macro event filter in scenario 4 at different target velocities. Potholes are marked by squares and poor road quality is marked by a bold line. The thin blue line represents the trajectory measured by the GPS.

We note that in figure 7.8(b) the macro filter marks almost the full trajectory with a deviation on the y-axis and z-axis. This was not expected, and the interpretation of this will be discussed in section 8.1.3. Apart from this, the filter finds the relevant sections, as marked in figure 3.5.

8. Discussion

In this section we will discuss the interpretations and implications of the results observed in the previous section. First we will discuss each filter in its own aspect and finally we will discuss the overall filter solution.

8.1 Evaluating Filter Components

8.1.1 The Kinematics Filter

The velocity $\bar{v}$ and the acceleration $\bar{a}_{center}$ are both based on the kalman estimates obtained by the GPS input $\bar{r}$. The outliers that are seen in the velocity and the acceleration curve of $\bar{a}_{center}$ are suggested to be a result from estimating a high frequency quantity from a low frequency data set. As is seen in the vector plot (figure 7.1), the estimates are feasible. However, they do not align with their true quantities sufficiently well. The outliers in the velocity curve (figure 7.2) were found to occur when the vehicle changes direction significantly. When the sample rate is too low there may be a significant difference in heading between two sample points, in particular when a sharp turn is made. Instead of a smooth gradual change of heading, the system models the kinematics by a small set of points implying great changes. These outliers are thus suggested to be a consequence from the system compensating a too low sample rate on the input. Furthermore the deviation from the intended average velocity is seen to be greater when the velocity is large, which also may be interpreted as a defect caused by a too low sample rate. These observations suggest that the sample rate of the input is insufficient for the statespace model used in the Kalman observer, which renders the model inaccurate. Our conclusion is that the results could be improved in two fundamentally different ways; either by adjusting the algorithms or by enhancing the indata.

One possible way of improving the algorithm is to increase the order of the interpolation. This would demand a larger delay on the overall system as more data points need to be considered when making a higher order interpolation. Another possible way would be to investigate a more sophisticated state space model for the Kalman observer, which most likely would turn out to introduce more lag or even a non-linear model. Considering Nyquists sampling theorem, such improvements on the algorithms may still be limited in their capabilities due to the low sample rate on $\bar{r}$. Furthermore, it is likely that these alternatives would increase the complexity of the algorithm. This is undesirable if the system is intended to run online locally on the TEM, as the hardware is limited in its computational capabilities.

In the currently implemented system, we obtain eight output quantities by measuring only two quantities. A consequence of this is that the output terms are strongly dependent on each other, and errors will propagate between terms in the model. In particular, errors within estimates based on the position measurements will propagate into terms derived from them. For example, the quantity $\bar{a}_{rotation}$ is expected to have a very small amplitude, as the main dynamics of the car is not of rotational nature. It is suggested that the unfeasible results of $\bar{a}_{rotation}$ is a consequence of errors within the term $\bar{a}_{center}$.

These errors are likely to have an amplitude which is in orders of magnitude greater than $\bar{a}_{rotation}$ itself. The outliers present in the velocity (as seen in figure 7.2) are also probable to be a consequence of errors arrising from estimates based on a too low sample rate in the position measurement.

Thus we suggest that the best way to improve the results from the kinematics filter is to improve the hardware. By providing high frequency measurements of relevant quantities so that he outputs can be identified more or less independently from each other, the system is likely to perform better. One such extension would be to add a high frequency gyroscope sensor, measuring rotations. This setup would make it possible to implement a dead reckoning system. In a dead reckoning system relative changes of the system are calculated based on high frequency measurements, so that the current state of the vehicle can be determined. The accumuated errors of the calculated current state can be corrected by sensor fusion of absolute measurements at a lower sample rate whenever these are available.

8.1.2 The Micro Event Filter

The micro event filter is considered to perform well, in spite of the poor performance of the kinematics filter. Invalid warnings are rare and only encountered when the external disturbances are considerable. Considerable in the sense that the magnitude of the random disturbances approaches that of the feature we are trying to identify. Since the behaviour of the vehicle is strongly irregular when affected by such disturbances, these invalid warnings are considered to be particularly hard to fully elimininate. It is suggested that the most effective way to improve the micro filter is to improve the estimate of $\bar{a}_{center}$. The motivation for this is that ideally $\bar{a}_{center}$ should contain only the center of mass acceleration, which is precisely the physical quantity that we are interested in.

8.1.3 The Macro Event Filter

The macro event filter is considered to perform sufficiently well. We note that the macro filter currently only provides decisional support for analysis on road conditions. For a final product, an external software that can collect, merge and interpret the obtained warnings from several cars is required. Such a software is likely to be running on a server and hence considered out of scope for this report.

An unexpected behaviour of the filter was found in figure 7.8(b), showing the result of scenario 4 at a target velocity of 50 km/h. Here we observed that the filter found large vibrations on the y-axis and z-axis. As the scenario contained several sharp turns, the car had to be driven at a low gear and high rpm in order to maintain the intended average velocity. It is proposed that this driving behaviour induced strong vibrations from the car engine to the car chassi. Thus setting off macro filter events, even though the road conditions were good. Interpreting high rpm of the engine as aggressive driving behaviour, this may be an interesting observation for future work.

8.2 Evaluating the Overall Solution

The current system is strongly dependent on the position measurement $\bar{r}$, as two of the most important estimates $\bar{v}$ and $\bar{a}_{center}$ are obtained through this sensor data. This is considered to be a major flaw in the current system for several reasons. It is likely that the GPS signal will be lost from time to time, for instance in tunnels. If the GPS signal is lost, the kinematic system cannot construct the intended output and as a consequence the filter collapses. Furthermore, it is concluded that the sample frequency of the GPS is too low for the proposed analysis.

9. Conclusions and Future Work

In this thesis we extended an existing generic M2M platform by implementing a filter software to interpret sensor data. The main purpose of the proposed kinematics filter is that it should model the kinematics of the vehicle, as this is considered to maintain the generic nature of the system solution. It is proposed that a wide variety of services can be developed based upon this output. As a proof of concept two filters that can interpret the output are implemented.

A model on how the kinematics of the car is related to the measured acceleration is formulated. By analyzing the acquired measurement data, it is found that the proposed model is suitable for the intended use. All filter implementations are tested and evaluated by applying them on measurement data obtained from actual scenarios. The conclusion from this is that services performing sufficiently well can be developed, even though the kinematics filter is considered to perform poorly.

9.1   Setting up Hardware

When analyzing data it is of utmost importance that the recieved input data is well defined. In section 3.1.2 we assumed that the hardware was calibrated and in section 4.2 we assumed that the reference frame of the TEM was perfectly aligned with the BF. These assumptions were necessary in order to interpret and analyze the acceleration within the scope of this thesis. In general those assumptions may not be valid. During the data acquisition phase of this thesis there were a lot of confusion and problems due to shortcomings of the hardware. A notable amount of time was consumed before it was discovered that the hardware units did not conform with their specifications. In particular a non uniform orientation of the accelerometer sensors was discovered, some units were not aligned with the markings on the hardware.

If the deviations and shortcomings of the hardware are known, most such problems can be handled by software. In this thesis project the particular problems was solved by using only one well known and tested unit. In future applications it is suggested that one should demand some guarantee of uniformity between units, for instance by a suitable ISO certification of the manufacturer. This will not necessarily eliminate errors, but it will ensure that potential errors are uniform in their appearance.

Problems related to the physical installation of the TEM may also provide problems, even when the hardware is uniform. To analyze the data as described in this thesis it may be necessary to know the rotation matrix transforming the acceleration data to the BF. It is suggested that the most robust way to handle this is to implement an automatic calibration software. In its simplest form it should identify the orientation of the TEM relative to the car. A more sophisticated version should also ensure that the sensor data is orthonormal.

9.2 Improving the Results

9.2.1 Current Shortcomings

A robust system should be able to handle data loss to some extent. If some sensor data is crucial for the system, it must provide a reliable stream of data at all times and never fail. This is certainly not the case with a GPS, as it may lose contact with satellites. Furthermore the precision depends not only on the hardware but also on the current spatial configuration of the satellites. High frequency micro sensors such as accelerometers, assuming that they are properly calibrated, is a more reliable source of data. As described in [9], the dynamics of a rigid body such as a car is determined by the acceleration and angular rates of the body. It is found in [10] that the angular rates can be determined by a set of at least six, but prefereably nine linear accelerometers. Though it is also concluded by [10] that a more suitable setup is to combine the sensor data of an accelerometer and a gyroscope to determine the angular rate.

9.2.2 Dead Reckoning and Sensor Fusion

Using the GPS to reconstruct the kinematics of the vehicle was found to be problematic for several reasons. As discussed in section 8.1.1, this GPS data is sampled at a very low frequency. As a consequence of the low sampled data the reconstruction filter performed poorly. In this section we will describe an alternative concept on how to reconstruct the kinematics.

Sensors can be said to be either relative or absolute. An accelerometer and a gyroscope are relative in the sense that they cannot determine the initial position of a body, but they can be used to determine how a body's position and orientation varies over time relative to the initial state. In the same way, a GPS is absolute in the sense that it can determine the bodys position independently of the intitial state. A dead reckoning system uses a suitable model to calculate the current state of a system, based on information from relative sensors. No model is perfect, of course, so there will be an accumulated drift in accuracy over time. To handle this drift in accuracy, the state of the dead reckoning system could be corrected by sensor fusion from absolute sensors. A navigation system of this type is proposed to have several advantages over the currently implemented filter solution.

Relative sensors are often reliable and accurate in their performance, and usually samples at a high frequency. Provided that the accumulated drift is corrected by absolute sensor data when necessary, the kinematics may be reconstructed with a high resolution and accuracy. Since the state estimation of a dead reckoning system is based upon relative sensors, the system may operate even when the GPS signal is lost. The current system would fail completely if the GPS signal is lost, whereas a dead reckoning fusion system would be able to maintain functionality although at a decreased accuracy. Furthermore, it is proposed that under normal conditions when all sensor data is available, a dead reckoning fusion system is likely to provide more accurate results.

9.2.3 Suggested Improvements on the Hardware

In order to implement a dead reckoning fusion system, the hardware must be extended with a suitable set of sensors. Even if the TEM is computationally capable of analyzing data locally, it must be extended with more sensor data in order to provide the information necessary for an accurate model of the kinematics. The relative quantities that we would like to measure is the acceleration and the angular rate of the body.

The hardware should thus be equipped with the following relative sensors:

- high frequency three axis accelerometer

- high frequency three axis gyroscope

Furthermore the hardware should be equipped with the following absolute sensors:

- high resolution clock

- GPS

With this sensor setup the physically relevant data could be sampled at a high frequency, and the low frequency position samples may be used to adjust and correct the calculated values. This is proposed to provide a sufficient range of sensor data to reconstruct the dynamics with a dead reckoning system.

Bibliography

[1] Harbor Research inc. 2011, Next Generation Platform Innovation In M2M [white paper]. Retrieved from http://www.verizonenterprise.com/resources/whitepapers/wp_next_generation_platform_ innovation_in_m2m_en-xg.pdf

[2] LogicIO, CX1 pro-c, http://www.logicio.com/rtcu_products.htm

[3] Albert Krohn et. al., Inexpensive and Automatic Calibration for acceleration Sensors, Telecooperation Office - Universität Karlsruhe, 2004.

[4] Reza N. Jazar, Vehicle dynamics - Theory and applications, Springer, third edition, 2009

[5] Oliver M. O'Reilly, Engineering dynamics: a primer, Springer, second edition, 2010, Chapter 8-9.

[6] Department of defense, World geodetic system 1984 - it's definition and relationships with local geodetic systems, National Imagery and Mapping Agency (NIMA), third edition, January 2000, section 2.

[7] Clynch James R., Earth coordinates, Retrieved from http://clynchg3c.com/Technote/geodesy/radiigeo.pdf

[8] Steven W. Smith, The Scientist and Engineer's Guide to Digital Signal Processing, California Technical Publishing, 2nd edition, 1999, chapter 15.

[9] David Baraff, An introduction ot physically based modeling, Carnegie Mellon University, 1997.

[10] Frere P.E.M, Problems with using accelerometers to measure angular rate in automobiles, Sensors and Actuators A: Physical, Volume 27, Issues 1–3, May 1991, Pages 819–824

[11] Defence mapping agency, The universal grids: Universal Transverse Mercator (UTM) and Universal Polar Stereographic (UPS), 1989, chapter 2.

[12] Chair of statistics, Time series analysis - Examples with SAS, University of Würzburg, version 2012.August.01, 2012, chapter 1-3.

[13] Clynch James R., Datums - Map coordinate reference frames, Retrieved from http://clynchg3c.com/Technote/maps/Datum_i.pdf

[14] Clynch James R., Earth coordinates, Retrieved from http://clynchg3c.com/Technote/geodesy/coorddef.pdf